Dalton Transactions

PAPER

View Article Online
View Journal | View Issue



Cite this: *Dalton Trans.*, 2019, **48**, 15567

# Design and photophysical studies of iridium(III)–cobalt(III) dyads and their application for dihydrogen photo-evolution†

Cédric Lentz, [a] Olivier Schott,[b] Thomas Auvray, [b] Garry S. Hanan *[b] and Benjamin Elias *[a]

Received 13th May 2019,
Accepted 16th July 2019

DOI: 10.1039/c9dt01989h

rsc.li/dalton

We report several new dyads constituted of cationic iridium(III) photosensitizers and cobalt(III) catalyst connected *via* free pendant pyridine on the photosensitizers. These dyads were studied by X-ray crystallography, electrochemistry, absorption and emission spectroscopy as well as theoretical calculations and were shown to efficiently produce $H_2$ under visible light irradiation. In every case, the dyad outperformed the equivalent system without a pendant pyridine. The dependence between irradiation wavelength and photocatalytic performances was also studied, with $H_2$ being evolved with turn-over numbers up to 295, 251, 188 and 78 $mol_{H_2}$ $mol_{PS}^{-1}$ under blue, green, yellow and red light, respectively.



## Introduction

Sunlight conversion into usable forms of energy is the ideal alternative to fossil fuels, and photovoltaic cells have been developed to such ends.[1] However, one of the main disadvantages of such systems is the efficient storage of the energy produced. As a result, new solar energy conversion systems that can convert light into chemical energy may improve the energy storage efficiency. The most promising approach towards this goal is the conversion of solar energy into storable fuels such as molecular hydrogen.[2] Hydrogen evolution reaction (HER) systems require a photosensitizer (PS), a catalyst, a source of protons, and, in the case of half-reactions, a sacrificial electron donor; and the electronic properties of each unit need to be optimized. In addition, the way the different units of the HER system are connected should always minimize the risk of charge recombination processes, which decrease the overall efficiency of the systems. Thus, several studies aimed at the development of mono-component photocatalysts[3] as they show better efficiency in terms of electron transfer compared to the related multicomponent systems.[3b,e,4]

The focus of many research groups for the past decades has been the development of hydrogen-evolving molecular catalysts with earth-abundant metals[5] such as Ni,[6] Co,[6c,7] Fe,[8] Cu[9] or Mo[7j,10] instead of Pt,[4a,c,11] Rh[12] or Pd.[3a,11i,13] We chose to use cobaloximes because they combine high efficiency in the HER with ready availability. As coordination of the PS to the Co catalyst is known to influence the catalytic activity of the Co(III) centre and to enhance its stability, we included this into the design of our system.[14]

The PS unit has also been based on a variety of metal ions, the most common being Ru,[14,15] Re[16] and Ir.[3b,4a,8f,11c,12e,17] Cationic cyclometalated Ir(III) complexes, although well-known for their moderate to high cost, present several advantages over first row transition metals, due to their higher tunability upon small variation of the first coordination sphere. Previous studies have shown that such Ir(III) complexes, even if their light absorption properties do not span over the all visible range, outperform archetypal PS such as $[Ru(bpy)_3]^{2+}$ (bpy = 2,2′-bipyridine) in $H_2$ photo-production.[3b,4f]

Bernhard and co-workers studied the influence of fluorine atoms on the cyclometalated ligands of $[Ir(ppy)_2(N^N)]^+$ (ppyH = 2-phenylpyridine) derivatives and found out that the obtained complexes displayed a higher luminescence quantum yield as well as a blue-shifted emission associated to a slightly more efficient $H_2$ photoproduction compared to non-fluorinated derivatives.[4f,18] In contrast, Huang and co-workers showed that using 1–phenylisoquinoline (piqH) as the cyclometalated ligand provides an enhanced conjugation of the system causing a higher molar absorptivity of the

[a]*Institute of Condensed Matter and Nanosciences, Molecular Chemistry, Materials and Catalysis Division (IMCN/MOST), Université catholique de Louvain, Place Louis Pasteur 1, bte L4.01.02, 1348 Louvain-la-Neuve, Belgium. E-mail: benjamin.elias@uclouvain.be*

[b]*Département de Chimie, Université de Montréal, 2900 Boulevard Edouard-Montpetit, Montréal, Québec H3T 1J4, Canada. E-mail: garry.hanan@umontreal.ca*

†Electronic supplementary information (ESI) available: Synthetic procedures, data for cyclic voltammetry, absorption, emission, acid titration theoretical model parameters and results, crystallographic study and hydrogen evolution setup. CCDC 1851560, 1851595 and 1851608. For ESI and crystallographic data in CIF or other electronic format see DOI: 10.1039/c9dt01989h

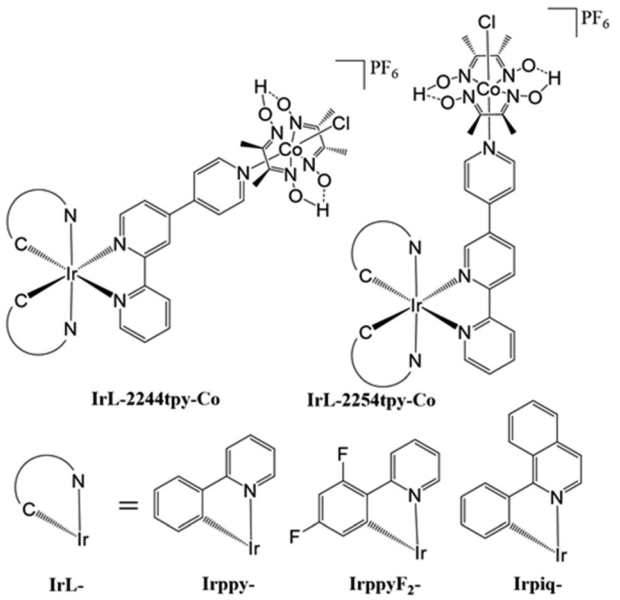


**Chart 1** Structure and abbreviations of the **[Ir–Co]** dyads.

Ir(III) core as well as red-shifted absorption compared to 2-phenylpyridine.[19]

We recently reported that an **[Ir–Co]** dyad using piqH as cyclometalating ligand could efficiently photo-evolve $H_2$, even under red light irradiation.[17d] In this work, we aimed to study the $H_2$ photoproduction of six different Ir(III)–Co(III) dyads (Chart 1). To this end, two different terpyridines *i.e.* 2,2′;4′,4″-terpyridine (2244tpy) and 2,2′;5′,4″-terpyridine (2254tpy) were used as bridging ligands. Indeed, despite their apparent similarity, both bridging ligands display different electron density on the pendant pyridine moiety leading to different photophysical properties (*vide infra*). To maximize the activity of the **[Ir–Co]** dyads, different cyclometalating ligands were used as well; 2–phenylpyridine, 2-(2′,4′-difluorophenyl) pyridine ($ppyF_2H$) and 1-phenylisoquinoline. Thus, we report herein the synthesis and study of six novel photoactive **[Ir–Co]** dyads with distinctive features in order to study the variation of their performances in photo-induced $H_2$ evolution under different wavelengths of light.

## Results and discussion

### Synthesis

The binuclear **[Ir–Co]** dyads were prepared in good yields as shown in Scheme 1. Both 2244tpy and 2254tpy were obtained after a Suzuki reaction between 4-pyridylboronic acid and 4-bromo-2,2′-bipyridine or 5-bromo-2,2′-bipyridine, respectively. The two latter precursors were obtained according to procedures described in the literature (see ESI†).[20] Both ditopic ligands were chelated onto the iridium dimer precursors (with ppyH, $ppyF_2H$ or piqH as cyclometalated ligand) in ethylene

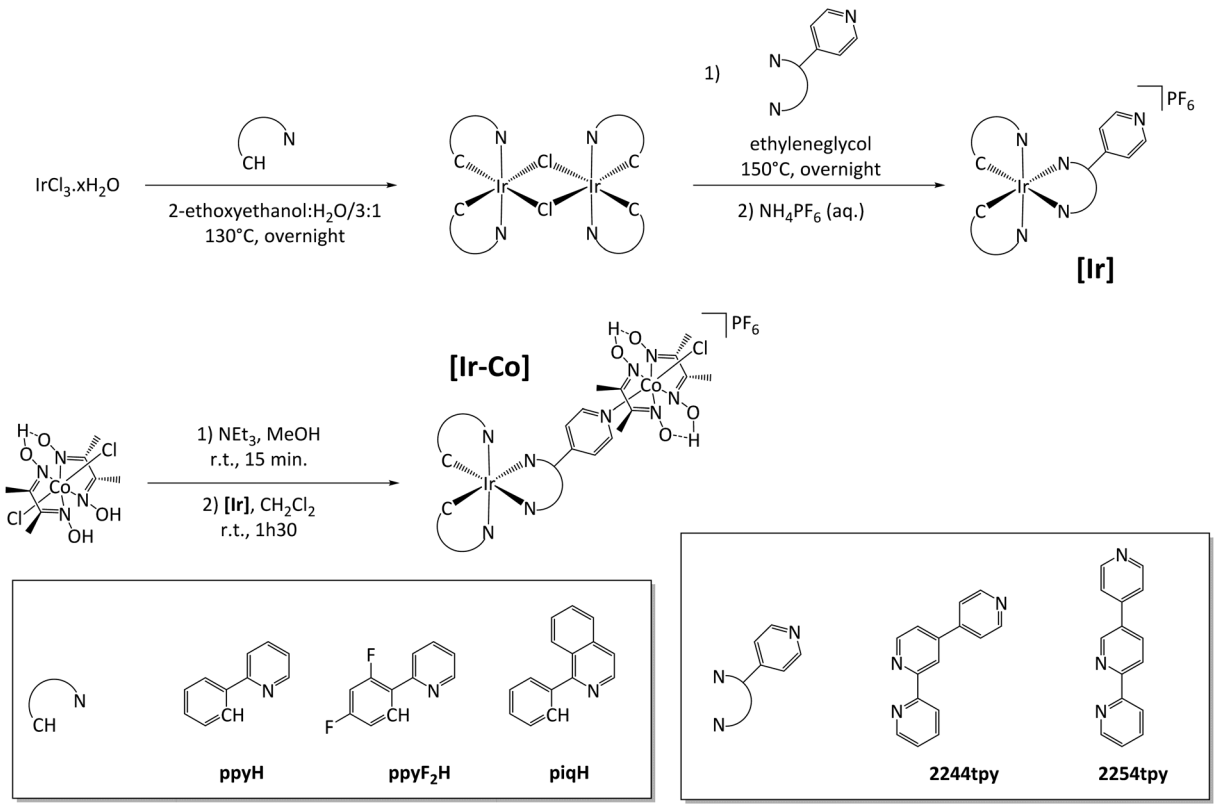


**Scheme 1** Synthetic procedure for the **[Ir–Co]** dyads.

 

glycol. The resulting complexes, referred as **[Ir]** in Scheme 1, were pure without any further purification. The dyads **[Ir–Co]** were obtained by subsequent chelation of the cobalt precursor $Co(dmgH)(dmgH_2)Cl_2$ on the pendant pyridine of the complexes **[Ir]** in a $CH_2Cl_2$ : MeOH/1 : 1 mixture in presence of $NEt_3$. This synthetic pathway presents a huge advantage as the reaction medium is close to the one used for $H_2$ photoproduction experiments, leaving the possibility of tuning both metallic centres separately and associating them subsequently *in situ* for the experiment (*vide infra*). Ir(III) photosensitizers with a bpy ligand were also synthesized in the same way as **[Ir]** for control $H_2$ photoproduction studies with multicomponent systems.

In the $^1$H NMR spectroscopy (see Fig. S1–15†), the multiplicity and coupling constants of each proton could not be determined due to the superposition of several peaks and/or lack of fine resolution for some signals. However, the $^1$H NMR spectra showed unambiguously the absence of symmetry elements for the IrL-2244tpy and IrL-2254tpy complexes (IrL- = Irppy-, Irppy$F_2$- and Irpiq-) and corresponding **[Ir–Co]** dyads, which induces the non-equivalence of the protons of (i) the extended N^N ligand and (ii) the ancillary ligands.

### Crystallographic studies

The slow diffusion of diisopropyl ether into distinct acetonitrile solutions of Irppy-2244tpy, Irppy-2245tpy and Irpiq-2254tpy at room temperature led to the growth of crystals suitable for X-ray diffraction analysis, with the $C_2/c$, $P2_1/c$ and $C_2/c$ space groups, respectively (see Table S1† for the structure parameters).

The Ir coordination sphere in all cases exhibits similar environments to complexes previously reported such as **Irpiq-2254tpy-Co**,[17d] **Ir-bpy**[21] and **Irpiq-bpy** (see Tables S2 and S3†).[22] The twist angles between the pendant pyridine plane and the coordinated 2,2′-bipyridine plane in the 2244 and the 2254 isomers are 39.1° and 34.4°, respectively, which are similar to those of Ru[23] and Ir[3c,17d] derivatives. **Irpiq-2254tpy** and both structures **Irpiq-2254tpy-Co and Irpiq-2254tpy-Co** show 25.6°, 31° and 27.9° between the planes of the 5,4 sites. Angles between chelating[17c] bipyridines of the 4-isomer terpyridine approaches planarity with 1.9° *vs.* 6.2° for the 5-derivative (see Tables S2 and S3†). The Ir-to-N (pendant pyridine) distance is 9.196(7) Å in the 4-isomer and 8.124(3) Å in the 5-isomer (Fig. 1a and b). In the **Irpiq-2254tpy-Co**, the distance between Ir and Co centers is 9.8666(8) Å. The crystal structure of the analogue Ir-Cobaloxime dyad with terpyridine Ir derivative shows 10.827 (1) Å between two metallic centres.[17c] The environment of Co with the bond length N(pyridine)–Co 1.966(2) Å (Fig. 1c) is similar to the analog dyad[17c] and pyridyl derivatives of mononuclear cobaloximes such as $Co(dmgH)_2ClPyr$[24] (1.959 Å) and $Co(dmgH)_2(4\text{-}CNPy)Cl$[25] (1.963 Å).

### Electrochemical properties

The electrochemical data for all the Ir(III) complexes and Ir(III)–Co(III) dyads were obtained by cyclic voltammetry in dry deoxygenated acetonitrile.[3a,c,4e,26] The voltammograms are illustrated in the ESI (Fig. S21–S36†) while the values are reported in Table 1.

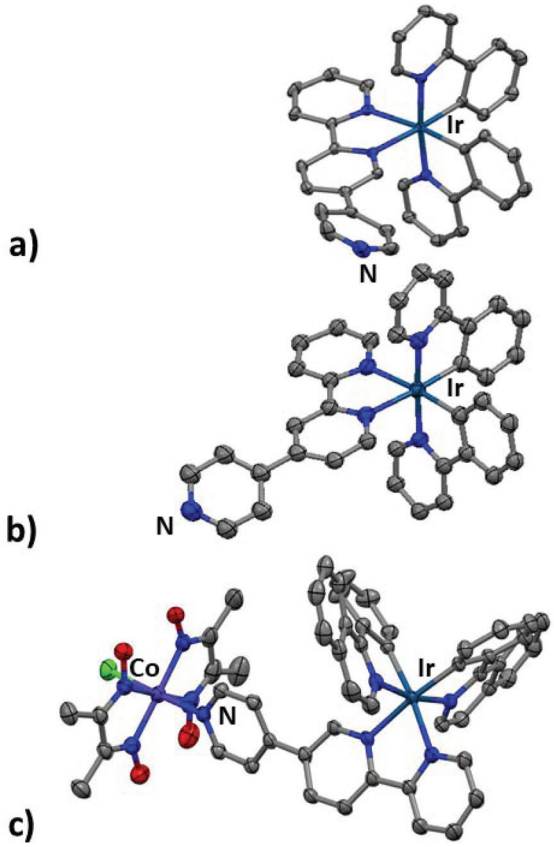


**Fig. 1** X-Ray structures of (a) Irppy-2245tpy, (b) Irppy-2244tpy (c) Irpiq-2254tpy-Co. The nitrogen of the pendant pyridine is highlighted in the three structures. Ellipsoids are at the 50% probability level. H atoms, $PF_6$ counter anions, and co-crystallized solvent molecules are omitted for clarity.

All the Ir based complexes display only one oxidation wave in the investigated electrochemical window. Irppy$F_2$-N^N complexes display an anodically-shifted oxidation wave compared to Irppy-N^N and Irpiq-N^N complexes ($E_{ox,IrppyF2\text{-}N\^N}$ = 1.72 V while $E_{ox,Irppy\text{-}N\^N} \approx E_{ox,Irpiq\text{-}N\^N}$ = 1.37–1.43 V *vs.* Ag/AgCl) due to the electron-withdrawing effect of the fluorine atoms. The oxidation process occurs on the Ir(III)-cyclometalated ligands fragment of the photosensitizers, irrespective of the nature of the N^N ligand. This attribution is confirmed by our DFT calculations (B3LYP/6-31G* and VDZ-SBKJC for Ir) showing that the HOMO has a mixed contribution of the metal (40%) and the phenyl part of the cyclometalated ligands (60%) (see Tables S6–S16†).

In the case of the dyads, chelation of the Co(III) center on the pendant pyridine does not affect the oxidation potential of the complexes, as expected since there is no contribution of this pyridine of the complex in the HOMO level. This is also showing the absence of communication between the two metal centres.

**Table 1** Electrochemical data for the Ir(III) photosensitizers and corresponding **[Ir–Co]** dyads measured in acetonitrile solutions with 0.1 M in TBAP at 25 °C[a]

| Complex | $E_{ox}$ | $E_{red}$ | | | | |
|---|---|---|---|---|---|---|
| Irppy-2244tpy | 1.37 (99) | | | −1.17 (100) | −1.72 (106) | |
| Irppy-2254tpy | 1.37 (149) | | | −1.11 (198) | −1.62 (207) | |
| Irppy-bpy | 1.37 (129) | | | −1.30 (111) | | |
| $IrppyF_2$-2244tpy | 1.72 (138) | | | −1.17 (86) | −1.72 (111) | |
| $IrppyF_2$-2254tpy | 1.72 (129) | | | −1.06 (134) | −1.53 (166) | |
| $IrppyF_2$-bpy | 1.71 (184) | | | −1.25 (169) | | |
| Irpiq-2244tpy | 1.42[b] | | | −1.16 (108) | −1.64 (114) | −1.86 (135) |
| Irpiq-2254tpy | 1.43[b] | | | −1.09 (124) | −1.60 (173) | −1.75 (131) |
| Irpiq-bpy | 1.36 (156) | | | −1.30 (128) | −1.67 (104) | |
| Irppy-2244tpy-Co | 1.45[b] | −0.44[b] | −0.97 (128) | −1.14 (88) | −1.71 (96) | |
| Irppy-2254tpy-Co | 1.46[b] | −0.44[b] | −0.95 (128) | −1.10 (71) | −1.56 (76) | |
| $IrppyF_2$-2244tpy-Co | 1.67 (147) | −0.40[b] | −0.96 (98) | −1.08 (76) | −1.64 (85) | |
| $IrppyF_2$-2254tpy-Co | 1.69 (144) | −0.44[b] | ≈−0.95[c] | −1.49 (80) | | |
| Irpiq-2244tpy-Co | 1.43[b] | −0.42[b] | −0.95 (90) | −1.13 (86) | −1.62 (43) | −1.81 (94) |
| Irpiq-2254tpy-Co | 1.43[b] | −0.43[b] | −0.95 (71) | −1.09 (75) | −1.55 (110) | −1.73 (77) |

[a] Potentials in V *vs.* Ag/AgCl, sweep rate of 100 mV $s^{-1}$. The difference between cathodic and anodic peak potentials (millivolts) is given in parentheses. [b] Irreversible; potential is given for the cathodic wave. [c] Overlapping of Co and ligand reductions giving a broad unresolved wave.

When looking at the reduction of the Ir complexes, several waves were observed. The first reduction takes place on the N^N ligand, and, as expected, the IrL-2244tpy and IrL-2254tpy series are easier to reduce than the IrL-bpy series ($E_{red,IrL\text{-}2244tpy} \approx -1.17$ V; $E_{red,IrL\text{-}2254tpy} \approx -1.09$ V; $E_{red,IrL\text{-}bpy} \approx -1.28$ V *vs.* Ag/AgCl) due to the extended conjugation of the ditopic ligand. The second reduction process corresponds to the reduction of the pyridine moiety. Irpiq-N^N complexes display a third reduction wave corresponding to the reduction of the isoquinoline part of the ancillary ligand.[19b]

When the Co(III) core is chelated to IrL-2244tpy or IrL-2254tpy, two new reduction processes are observed at ≈−0.42 V and ≈−0.96 V *vs.* Ag/AgCl corresponding to irreversible Co(III)/Co(II) and reversible Co(II)/Co(I) reductions, respectively. Using the ground state potentials and the energy of the excited state corresponding to the maximum of the emission spectrum at 298 K in acetonitrile (*vide infra* and Table S4†), the estimated potential in the excited states (namely $E^*_{ox}$ and $E^*_{red}$) are gathered in Table S5.†

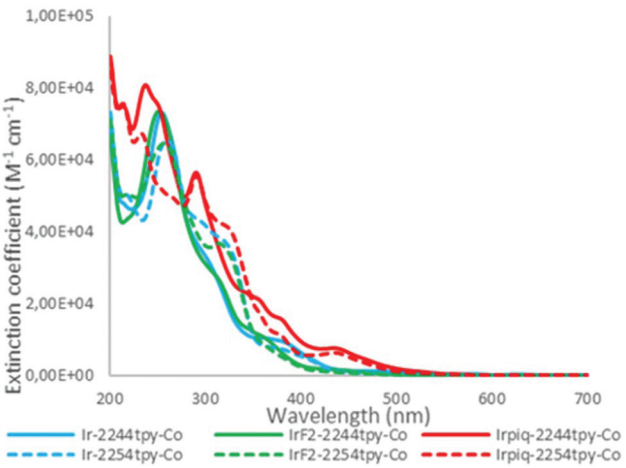


**Fig. 2** Absorption spectra of **[Ir–Co]** dyads in acetonitrile.

### Absorption spectroscopy

Fig. 2 displays the UV-visible absorption spectra for the six Ir(III)–Co(III) dyads in acetonitrile while the values are reported in Table 2 (absorption spectra and numerical values for all Ir(III) photosensitizers are in Fig. S16–S18 and Table S4 of the ESI†). All the compounds display absorption bands in the UV region tailing into the visible (Table 2).

On the basis of previous studies on cyclometalated Ir(III) complexes and the absorption of the ligands, intense absorption bands in the UV region can be ascribed to ligand-centred (LC) transitions.[27] On the other hand, absorption bands appearing in the visible region correspond to a complex mix of LC transitions and charge-transfer transitions from the cyclometalated ligand to the N^N ligand (inter ligand charge transfer – ILCT) or from the Ir centre to one of the ligand (metal to ligand charge transfer – MLCT). From our TD-DFT calculations on the nine Ir complexes, we could determine the contribution for each transition below 300 nm (see Tables S21–S29†), our model matching well with the experimental data as shown in Fig. S78–92.† Due to the previously discussed mixed contribution from both the metal and the cyclometalated ligand on several orbitals, many transitions are described as a combination of charge transfer from the metal and the C^N ligand towards the N^N ligand, thus having MLCT(N^N) and ILCT characters. We will refer to these transitions as a metal–ligand-to-ligand charge transfer (MLLCT) thereafter. In a similar way, several unoccupied levels have contributions from both type of ligands, leading to transitions being described as both MLLCT resulting in population of orbitals on the N^N ligand and a mix of MLCT and LC populating orbitals on the C^N ligand.

The energies of the transitions in the visible region of $IrppyF_2$-N^N complexes (N^N = 2244tpy, 2254tpy and bpy) are

 

Table 2 Spectroscopic data for the [Ir–Co] dyads[a]

| Complex | $\lambda_{abs}$ [nm] ($\varepsilon$ [×10$^2$ M$^{-1}$ cm$^{-1}$]) | $\lambda_{max\ em}$ [nm] | $\tau^b$ [μs] | $\Phi^c$ (Ar) | $k_r{}^d$ [×10$^3$ s$^{-1}$] |
|---|---|---|---|---|---|
| Irppy-2244tpy-Co | 254 (731), 308 (291), 383 (92), 412 (44), 468 (12), 495 (10) | 652 | 0.035 (16%) 0.213 (84%) | 0.0030 | 16.3 |
| Irppy-2254tpy-Co | 215 (485), 260 (654), 294 (431), 326 (350), 377 (75), 409 (43), 468 (7), 514 (4) | 661 | 0.034 (11%) 0.115 (89%) | 0.0015 | 14.1 |
| IrppyF$_2$-2244tpy-Co | 252 (736), 312 (273), 343 (133), 360 (108), 420 (18), 445 (14) | 567 | 0.121 (14%) 0.384 (86%) | 0.0124 | 35.7 |
| IrppyF$_2$-2254tpy-Co | 258 (645), 315 (367), 331 (298), 361 (86), 421 (11), 448 (7) | 572 | 0.196 (13%) 0.406 (87%) | 0.0094 | 25.2 |
| Irpiq-2244tpy-Co | 215 (747), 238 (807), 251 (747), 291 (562), 339 (234), 355 (211), 380 (155), 437 (75), 528 (9), 567 (2) | 593, 637 | 1.053 | 0.0023 | 2.2 |
| Irpiq-2254tpy-Co | 215 (750), 235 (664), 291 (554), 327 (398), 357 (180), 379 (111), 437 (62), 530 (5), 567 (2) | 593, 637 | 0.705 | 0.0033 | 4.7 |

[a] Measurements in degassed acetonitrile at 298 K. [b] Lifetime under $N_2$ atmosphere. [c] Quantum yield measured by using $[Ru(bpy)_3]^{2+}$ as a reference, $\Phi_{ref}$ = 0.028 in water under air. [d] Radiative rate constant determined under an inert atmosphere at 298 K ($k_r = \Phi/\tau$).



blue-shifted compared to those of corresponding Irppy-N^N complexes due to the electron-withdrawing behaviour of the fluorine atoms which stabilizes the HOMO of the complexes (see Fig. S76†). On the other hand, the higher conjugation of Irpiq-N^N complexes due to the additional fused aromatic ring on the cyclometalated ligands stabilizes the system, leading to a slight redshift in absorption compared to Irppy-N^N complexes.

When comparing the absorption spectra of the complexes in each IrL-N^N family, one can observe that there are no major differences in the position and intensities of the absorption maxima in the visible region besides a slightly higher extinction coefficient for IrL-2244tpy relative to those with IrL-2254tpy, except around 320 nm where the IrL-2254tpy compounds present an additional shoulder. Based on the TD-DFT results, this feature is caused by an additional LC contribution from the N^N ligand to the transitions around 320 nm. This situation is favoured by the fact that the complexes based 2254tpy have mixed N^N and C^N contributions in the LUMO+2/+3, with varying ratio, while these levels are purely C^N for all the IrL-2244tpy family (see Tables S9 and S10† for example).

The lowest singlet transition in all cases has an MLLCT character. However, due the strong spin–orbit coupling of the Ir centre, there is significant mixing between the singlet and triplet states, allowing for spin forbidden triplet transitions to be directly excited. Thus, for the Irppy-N^N and IrppyF$_2$-N^N compounds, the lowest absorption bands around 500 and 450 nm, respectively, corresponds to a mixed $^{1/3}$MLLCT transition. However, for the Irpiq-N^N series, due to the extended conjugation of the cyclometalated ligand, there are several $^3$MLCT(C^N)/LC(C^N) transitions at lower energy than the mixed $^{1/3}$MLLCT transition.

Finally, it is noteworthy to mention that the absorption spectra for **[Ir–Co]** dyads are almost identical to those of the corresponding photosensitizers (see Fig. S34–39†) indicating that no strong electronic interaction occurs between the metallic centres, as observed in the electrochemistry study.

## Emission spectroscopy

The luminescence lifetimes and quantum yield of luminescence for each dyad and photosensitizer were measured in acetonitrile under an inert atmosphere (Tables 2 and S4,† respectively). While the Irppy-N^N and IrppyF$_2$-N^N series display broad unstructured emission spectra (Fig. S31–33†), as expected from $^3$CT-type excited states, more structured emission bands can be observed for the Irpiq-N^N series. This typical vibrational progression is implying a major $^3$LC contribution to the excited state of the Irpiq-N^N series in addition to the expected $^3$CT-type excited states. This interpretation is confirmed by the low temperature measurement, as the emission maxima are only slightly blue-shifted for the Irpiq-N^N series while the Irppy-N^N and IrppyF$_2$-N^N series show hypsochromic shifts of ≈−100 and ≈−40 nm respectively (Table S4†). It is also confirmed by the TD-DFT calculations showing that the lowest triplet state for Irppy-N^N and IrppyF$_2$-N^N is a $^3$MLLCT while it is a mix-state combing C^N centred $^3$MLCT and $^3$LC characters for Irpiq-N^N. Due to HOMO stabilization induced by the addition of fluorine atoms on IrppyF$_2$-N^N compounds, emissive transitions are more energetic compared to Irppy-N^N and Irpiq-N^N families. Despite the higher conjugation in the Irpiq-N^N family, the energy of the $^3$LC/$^3$CT transitions are quite close to those of the Irppy-N^N compounds.

It is noteworthy to mention that, in air-equilibrated solvents, a decrease in the luminescence intensity with respect to degassed solutions is systematically observed for every complex, indicating a quenching by oxygen. We expect that, as for Ir(III) complexes such as *fac*-[Ir(ppy)$_3$], an efficient photosensitization of $^3O_2$ by the excited Ir(III) complexes is occurring.[28] There is no significant difference between the IrL–2244tpy and IrL-2254tpy series. The emission maxima of the dyads in acetonitrile (Table 2) are close to those of the Ir(III) photosensitizers, exhibiting only a small red-shift falling within the limit of the resolution of our spectrometer. This indicates that the Co coordination does not lower significantly

the energy of the radiative pathways. Nevertheless, the observed decreased lifetimes and quantum yields imply that an intramolecular electronic or energetic transfer from the excited Ir unit to the Co unit takes place.

### Photochemical behavior upon addition of acid

We chose to study the effect of protonation on the pendant pyridine of our IrL-2244tpy and IrL-2254tpy complexes, as it has been shown by several groups to be an efficient way to probe the nature of the excited states. Indeed, if $^3$MLLCT transitions are predominant and the non-chelated pyridine is involved in the excited state, the corresponding absorption and emission energy should be altered by protonation.[29] Titration experiments were thus carried out in acetonitrile with two acids that have different p$K_a$ values, trifluoroacetic acid (TFA) (p$K_a$ = 12.65 in $CH_3CN$)[30] and acetic acid (AcOH) (p$K_a$ = 23.51 in $CH_3CN$).[31]

The luminescence quenching of IrL-2244tpy and IrL-2254tpy upon addition of trifluoroacetic acid as well as modifications of absorption bands are illustrated in the ESI (Fig. S40–63†). A clear red-shift of the most bathochromic band upon addition of TFA can be observed, which is consistent with the protonation of the pendant pyridine residue. On the other hand, no observable shift was noticed for the high energy absorption bands. The presence of several isosbestic points indicates the existence of two species in equilibrium. The emission of every complexes decreases dramatically with the addition of TFA, due to the additional non-radiative relaxation pathways created, especially by the repulsion between the positive charges. Interestingly, the luminescence quenching is quite similar for the complexes of a same family, *i.e.* IrL-2244tpy and IrL-2254tpy families showing the inertness of the cyclometalated ligands toward protonation. On the other hand, the measured luminescence quenching is more efficient for IrL-2254tpy complexes than for IrL-2244tpy due the electron-rich character of the 5′ position on the bpy residue with respect to 4′ position, which increases the basicity of the pendant 5′-pyridine of IrL-2254tpy complexes in the ground state. In the case of the Irpiq-N^N compounds, we discussed earlier that the emissive state was localized on the C^N ligand and thus should not be affected by the protonation. However, we observed a similar behaviour for the Irpiq-N^N complexes upon protonation, suggesting that the lowest excited state of the protonated form Irpiq-N^N-H$^+$ now has a $^3$MLLCT character. This is confirmed by the TD-DFT calculations on the protonated complexes (Tables S30–S35 and Fig. S77†).

The luminescence quenching of IrL-2244tpy and IrL-2254tpy upon addition of acetic acid are illustrated in the ESI (Fig. S64–S75†). It is noteworthy to mention that gradual addition of AcOH had no effect on the absorption of the complexes, even at high concentration implying that the pendant pyridine residue cannot be protonated in the ground state, as expected. Nevertheless, luminescence quenching could still be observed upon addition of AcOH taking advantage of contribution of the pendant pyridine on the LUMO for all the complexes, as observed in our DFT calculations. Interestingly, in contrast with the behaviour of the complexes in the presence of TFA, a strong acid, luminescence quenching of IrL-2244tpy complexes with gradual amounts of AcOH is more efficient than with IrL-2254tpy complexes. Indeed, due to the electron-poor character of the 4′ position of the bpy moiety compared to the 5′ position in the ground state, the excited electron will preferentially go to this position when the complex is irradiated, enhancing the electron density of the pendant 4′-pyridine. Furthermore, luminescence quenching due to protonation of the excited complexes is highly influenced by the nature of the ancillary ligands, due to the increasing contribution of the $^3$LC transition on the nature of the excited state ($^3LC_{Irppy\text{-}N^N} < {}^3LC_{IrppyF2\text{-}N^N} < {}^3LC_{Irpiq\text{-}N^N}$), leading to a less efficient $^3$MLLCT and, hence, a lower electron density in the excited state on the pendant pyridine residue, making Irpiq-2244tpy the least basic complex. The same observations are made for Irppy-2254tpy, Irppy$F_2$-2254tpy and Irpiq-2254tpy.

### Hydrogen photo-evolution

Based on the electrochemical and spectroscopic results discussed above, we investigated the light driven hydrogen evolution for the different complexes. We also wanted to confirm that the supramolecular assemblies were more efficient HER systems than their bimolecular counterparts, as we previously showed for **Irpiq-2254tpy-Co**.[17d] Thus, the Ir photosensitizers without pendant pyridines were tested with Co(dmgH)$_2$PyrCl in a 1/1 ratio of photosensitizer/catalyst as in the **[Ir–Co]** dyads prepared herein. As recent studies showed the dependence of photocatalytic activities *versus* the wavelength of irradiation, the compounds were analysed at various wavelengths to see the effect on the photoactivity.[17c,d]

Photocatalytic systems were analysed in acetonitrile with 0.5 M triethanolamine as the sacrificial electron donor and 0.05 M aqueous tetrafluoroboric acid as the proton source; the error associated with the TOF and TON values is estimated to be 10%.[17d] Four light-emitting diodes (LEDs), with emissions centred at 452, 525, 595 and 630 nm (see Fig. S93†), were used to evaluate the potential of photoredox processes for each system.[23] An overview of the results determines that the dissociated, bimolecular systems IrL-bpy/Co(dmgH)$_2$PyrCl are less efficient than mono component systems (Fig. 3 and Table 3). Spatial interactions between PS and catalyst through coordination bonding of pendant pyridine has been shown to enhance electronic transfers.[3b,e,17b,c,23,32] Indeed, it has been shown that fast electronic transfer from the reduced photosensitizer to the catalyst could lower the probability of decomposition of PS *via* ligand dissociation.[33] In the active photocatalytic system, a more robust HER catalyst leads to better performances of the photosensitizers. Compared to the photocatalytic activity of IrL-bpy/Co(dmgH)$_2$PyrCl reference system, **[Ir–Co]** dyads react faster under irradiation to reach a higher TON limited by the stability of cobaloxime.[17c]

The reference system Irppy-bpy/Co(dmgH)$_2$PyrCl attained a TON of 29 while the highest TON obtained in this study is ten times higher (for Irppy$F_2$-2254tpy-Co under blue light, TON = 290). The activity of cobaloxime gives its best performance

 

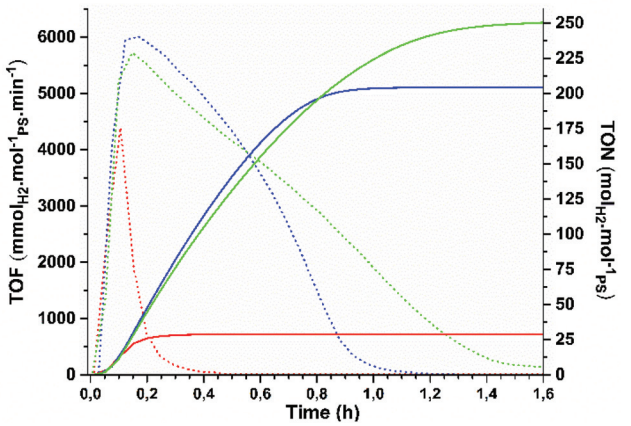


Fig. 3 Hydrogen evolution of Irppy-2244tpy-Co (blue), Irppy-2254tpy-Co (green) and dissociated system Irppy-bpy with Co(dmgH)$_2$PyrCl (red). Solid line: TON, dashed line: TOF. Blue LED irradiation centered at 452 nm (blue light).

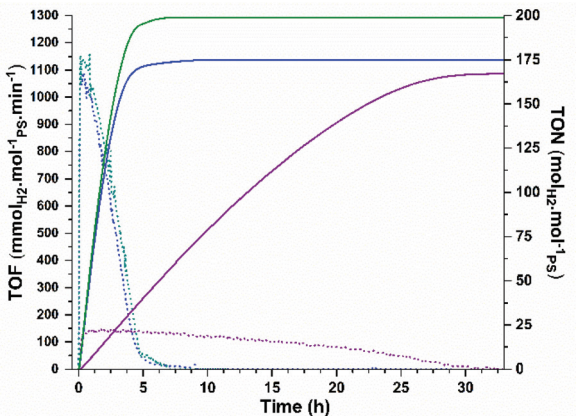


Fig. 4 Hydrogen evolution of Irppy-2244tpy-Co (blue), IrppyF$_2$-2244tpy-Co (purple) and Irpiq-2244tpy-Co (olive). Solid line: TON, dashed line: TOF. Irradiation centered at 525 nm (green light).

with the utilization of pyridyl pendant Ir photosensitizers. Under blue light irradiation, all PSs are excited in their absorption bands and generate photoredox processes. Irppy-2254tpy-Co displays higher activity than Irppy-2244tpy-Co *i.e.* TON of 250 and 200, respectively, and TOF$_{max}$ of 5700 mmol$_{H_2}$ mol$^{-1}$ min$^{-1}$ and 6000 mmol$_{H_2}$ mol$^{-1}$ min$^{-1}$, respectively (Fig. S94†). For IrppyF$_2$-derivatives, the TOF rate of IrppyF$_2$-2244tpy-Co is higher than IrppyF$_2$-2254tpy-Co, with 12 300 mmol$_{H_2}$ mol$^{-1}$ min$^{-1}$ *vs.* 8200 mmol $_{H_2}$ mol$^{-1}$ min$^{-1}$, respectively, but a lower TON is observed *i.e.* 260 (1.3 h) *vs.* 300 (2.8 h) (Fig. 4 and S96†). Irpiq-2254tpy-Co has a maximum rate of activity 16 000 mmol$_{H_2}$ mol$_{PS}^{-1}$ min$^{-1}$ with a TON = 180 (2.3 h), while Irpiq-2244tpy-Co displays a TON of 230 after 2.7 h and TOF$_{max}$ of 5200 mmol$_{H_2}$ mol$_{PS}^{-1}$ min$^{-1}$ (Fig. 3). The best performances in TOF and TON are attributed to the IrppyF$_2$- and Irpiq-derivatives. The former derivatives are known to generate a powerful oxidant in the excited state.[4f] The 1-phenylisoquinoline derivatives have been more investigated for their extension of electronic conjugation. In both series, a higher contribution of $^3$LC in the excited state is noticed and their excited-state lifetime is raised to the microsecond range. Those photophysical properties could be implicated in the efficiency of photoredox processes.[18,34] An interesting observation concerns the high efficiency of IrppyF$_2$-dyads under blue light irradiation even if tailing of their absorption spectra exhibit low absorption in the wavelength range of blue LEDs. It is noteworthy that under the same conditions dissociated systems display dramatically lower activities and sustainabilities compared to corresponding dyads. The Irppy-bpy and IrppyF$_2$-bpy systems quickly reach a TOF$_{max}$ of 4400 mmol$_{H_2}$ mol$^{-1}$ min$^{-1}$ and 4200 mmol$_{H_2}$ mol$^{-1}$ min$^{-1}$, respectively, followed by a rapid decreasing of activity to attain a modest TON of 29 (0.5 h) and 35 (0.8 h). The Irpiq-bpy/Co(dmgH)$_2$PyrCl system reacts much slower under blue light irradiation with a TOF$_{max}$ of only 350 mmol$_{H_2}$ mol$^{-1}$ min$^{-1}$ but with a more sustainable activity, with a TON of 71 is reached after 7 h (Fig. 3). Under green irradiation, the overlays of the absorption spectra of PSs and emission spectra of LEDs are weaker. As a result, the systems demonstrate lower activity. For dissociated system Irppy-bpy/Co(dmgH)$_2$PyrCl, a quick deactivation occurs to attain a TON of 16 (3.7 h) with a low TOF$_{max}$ of 180 mmol$_{H_2}$ mol$^{-1}$ min$^{-1}$ as

Table 3 Performances of photocatalytic systems under blue and green LEDs

| | Blue LED centered at 452 nm | | Green LED centered at 525 nm | |
|---|---|---|---|---|
| Compounds | TON | TOF$_{max}$ | TON | TOF$_{max}$ |
| Irppy-bpy/Co(dmgH)$_2$PyrCl | 29 (0.5 h) | 4400 | 16 (3.7 h) | 180 |
| Irppy-2244tpy-Co | 200 (1.5 h) | 6000 | 180 (9 h) | 1090 |
| Irppy-2254tpy-Co | 250 (1.7 h) | 5700 | 230 (12.8 h) | 1200 |
| IrppyF$_2$-bpy/Co(dmgH)$_2$PyrCl | 35 (0.8 h) | 4200 | 18 (27 h)[a] | 26 |
| IrppyF$_2$-2244tpy-Co | 260 (1.3 h) | 12 300 | 170 (30.3 h)[b] | 150 |
| IrppyF$_2$-2254tpy-Co | 290 (2.8 h) | 8200 | 150 (27.3 h) | 140 |
| Irpiq-bpy/Co(dmgH)$_2$PyrCl | 70 (7 h) | 350 | 30 (16 h) | 58 |
| Irpiq-2244tpy-Co | 230 (2.7 h) | 5200 | 200 (6.8 h) | 1200 |
| Irpiq-2254tpy-Co | 180 (2.3 h) | 16 000 | 250 (3.8 h) | 3500 |

TON in mol$_{H_2}$ mol$_{PS}^{-1}$. TOF in mmol$_{H_2}$ mol$_{PS}^{-1}$ min$^{-1}$. Induction time TON in mol$_{H_2}$ mol$_{PS}^{-1}$. TOF in mmol$_{H_2}$ mol$_{PS}^{-1}$ min$^{-1}$. [a] 15 min induction time. [b] 5 min of induction time.

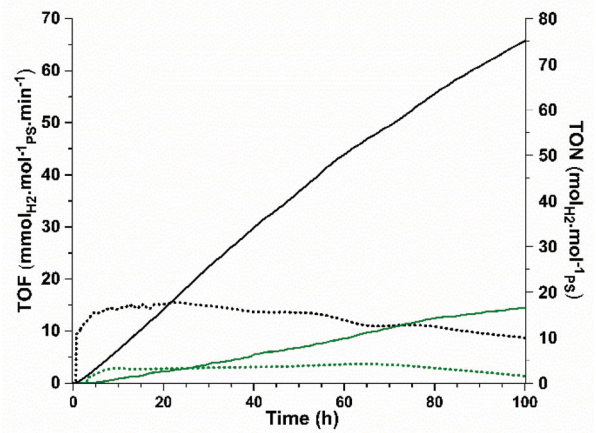


Fig. 5 Hydrogen evolution of Irpiq-2254tpy-Co (black) and Irpiq-2244tpy-Co (olive). Solid line: TON, dashed line: TOF. Irradiation centered at 630 nm (red light).

expected whereas Irppy-2244tpy-Co and Irppy-2254tpy-Co reach 180 (9 h) and 230 (12.8 h) with a TOF of 1100 and 1200 $mmol_{H_2}$ $mol_{PS}^{-1}$ $min^{-1}$, respectively (Fig. S98†). In the case of $IrppyF_2$-derivatives, weak absorptivity in the green range of the absorption spectra involves slow reactivity but high sustainability. Indeed, $IrppyF_2$-bpy/Co($dmgH_2$)PyrCl system maintains activity during 27 h with a low rate of 26 $mmol_{H_2}$ $mol_{PS}^{-1}$ $min^{-1}$. $IrppyF_2$-2244tpy-Co and $IrppyF_2$-2254tpy-Co produce a TON of 170 (30.3 h) and 150 (27 h) with a sustainable rate of 150 $mmol_{H_2}$ $mol_{PS}^{-1}$ $min^{-1}$ and 140 $mmol_{H_2}$ $mol_{PS}^{-1}$ $min^{-1}$, respectively (Fig. S99†). In the case of Irpiq-derivatives, multicomponent Irpiq-bpy/Co($dmgH_2$)PyrCl system displays a weak activity with a TON of 30 (16 h) with 58 $mmol_{H_2}$ $mol_{PS}^{-1}$ $min^{-1}$. The Irpiq-2254tpy-Co dyad demonstrates again a faster rate with 3500 $mmol_{H_2}$ $mol_{PS}^{-1}$ $min^{-1}$ to obtain a TON of 250 (3.8 h) *vs.* 1200 $mmol_{H_2}$ $mol_{PS}^{-1}$ $min^{-1}$ and 200 of TON (6.8 h) for Irpiq-2244tpy-Co (Fig. S97†). Under yellow LED irradiation, no production of dihydrogen is detected for all the dissociated systems. The Ir-2244tpy-Co and Ir-2254tpy-Co are active both for 110 h to reach a TON of 43 and 66, respectively. No production of hydrogen was detected for both $IrppyF_2$-2244tpy-Co and $IrppyF_2$-2254tpy-Co as expected because their absorption spectra cannot be superposed to the emission spectrum of the yellow LED (Fig. S100†). Irpiq-2244tpy-Co and Irpiq-2254tpy-Co generate a TON of 110 (43 h) and 180 (18 h) with a TOF of 66 $mmol_{H_2}$ $mol_{PS}^{-1}$ $min^{-1}$ and 265 $mmol_{H_2}$ $mol_{PS}^{-1}$ $min^{-1}$, respectively (Fig. S100†). The tailing of the absorption spectra for Irpiq-2254tpy displays a weak absorptivity until 590 nm *vs.* Irpiq-2244tpy at 560 nm. Under red LED centered at 630 nm, Irpiq-2254tpy-Co exhibits a slow constant hydrogen production for more than 100 h with a TON of 78,[17d] whereas a three-fold slower activity for Irpiq-2244tpy is detected (Fig. 5). Photoredox processes generated with low energy absorbed in the system could be enhanced by electronic communication between the photosensitizer and the catalyst. Indeed, the direct population of the lowest $^{1/3}$MLLCT excited at the tailing of absorption spectra drives a constant sustainable photoactivity.

## Conclusions

In each family of compounds, the bridging ligand tpy isomers based on the 4 and 5 position influence the photo-activity of the compounds. Irpiq-2254tpy-Co and $IrppyF_2$-2244tpy-Co exhibit the fastest photoredox processes of the study under blue light irradiation. Irppy-2254tpy-Co and Irpiq-2254tpy-Co are more productive than their homologous 4-isomers with the yellow and red irradiations in the tailing of their absorption spectra. Extending electronic conjugation with a phenylisoquinoline substituent in cyclometalated ligands permits hydrogen to be produced from red light irradiation. In Ru–Pd dyads, direct population of the lowest triplet excited state distributed on bridging ligands provides better stability of the system.[13b] In our system, the efficiency of photocatalysis under red light appears surprisingly efficient for the small absorptivity in the tailing of absorption spectra. We are currently investigating the impact of orbital contributions in electronic transitions implicated in photo-redox processes.

## Conflicts of interest

There are no conflicts to declare.

## Acknowledgements

This work was supported by the Fonds de la Recherche Scientifique – FNRS under Grant n° J.0091.18. B. E. and C. L. thank the UCLouvain and the Erasmus program for financial support. T. A., O. S. and G. S. H. thank the Direction des Affaires Internationales of UdeM. T. A. is grateful for scholarships from the Faculté des Arts et Sciences. G. S. H thanks the Natural Sciences and Engineering Research Council of Canada. This research was enabled, in part, by support provided by WestGrid and Compute Canada.

## Notes and references

1 R. F. Service, *Science*, 2005, **309**, 548–551.
2 N. Armaroli and V. Balzani, *ChemSusChem*, 2011, **4**, 21–36.
3 (*a*) S. Rau, B. Schafer, D. Gleich, E. Anders, M. Rudolph, M. Friedrich, H. Gorls, W. Henry and J. G. Vos, *Angew. Chem., Int. Ed.*, 2006, **45**, 6215–6218; (*b*) A. Fihri, V. Artero, A. Pereira and M. Fontecave, *Dalton Trans.*, 2008, 5567–5569; (*c*) A. Jacques, O. Schott, K. Robeyns, G. S. Hanan and B. Elias, *Eur. J. Inorg. Chem.*, 2016, **2016**, 1779–1783; (*d*) C. Li, M. Wang, J. Pan, P. Zhang, R. Zhang and L. Sun, *J. Organomet. Chem.*, 2009, **694**, 2814–2819; (*e*) A. Fihri, V. Artero, M. Razavet, C. Baffert, W. Leibl and M. Fontecave, *Angew. Chem., Int. Ed.*, 2008, **47**, 564–567; (*f*) N. Queyriaux,

 

R. T. Jane, J. Massin, V. Artero and M. Chavarot-Kerlidou, *Coord. Chem. Rev.*, 2015, **304–305**, 3–19; (*g*) W. T. Eckenhoff, *Coord. Chem. Rev.*, 2018, **373**, 295–316; (*h*) B. Zhang and L. Sun, *Chem. Soc. Rev.*, 2019, **48**, 2216–2264.

4 (*a*) D. R. Whang, K. Sakai and S. Y. Park, *Angew. Chem., Int. Ed.*, 2013, **52**, 11612–11615; (*b*) S. Hansen, M. M. Pohl, M. Klahn, A. Spannenberg and T. Beweries, *ChemSusChem*, 2013, **6**, 92–101; (*c*) K. Sakai and H. Ozawa, *Coord. Chem. Rev.*, 2007, **251**, 2753–2766; (*d*) A. N. Radhakrishnan, P. P. Rao, K. S. Linsa, M. Deepa and P. Koshy, *Dalton Trans.*, 2011, **40**, 3839–3848; (*e*) P. Zhang, P. A. Jacques, M. Chavarot-Kerlidou, M. Wang, L. Sun, M. Fontecave and V. Artero, *Inorg. Chem.*, 2012, **51**, 2115–2120; (*f*) J. I. Goldsmith, W. R. Hudson, M. S. Lowry, T. H. Anderson and S. Bernhard, *J. Am. Chem. Soc.*, 2005, **127**, 7502–7510.

5 K. E. Dalle, J. Warnan, J. J. Leung, B. Reuillard, I. S. Karmel and E. Reisner, *Chem. Rev.*, 2019, **119**, 2752–2875.

6 (*a*) N. A. Eberhardt and H. Guan, *Chem. Rev.*, 2016, **116**, 8373–8426; (*b*) Y. Han, H. Fang, H. Jing, H. Sun, H. Lei, W. Lai and R. Cao, *Angew. Chem., Int. Ed.*, 2016, **55**, 5457–5462; (*c*) Z. Han and R. Eisenberg, *Acc. Chem. Res.*, 2014, **47**, 2537–2544; (*d*) C. Tsay and J. Y. Yang, *J. Am. Chem. Soc.*, 2016, **138**, 14174–14177; (*e*) S. Wiese, U. J. Kilgore, M. H. Ho, S. Raugei, D. L. DuBois, R. M. Bullock and M. L. Helm, *ACS Catal.*, 2013, **3**, 2527–2535; (*f*) C. F. Wise, D. Liu, K. J. Mayer, P. M. Crossland, C. L. Hartley and W. R. McNamara, *Dalton Trans.*, 2015, **44**, 14265–14271; (*g*) H. N. Kagalwala, E. Gottlieb, G. Li, T. Li, R. Jin and S. Bernhard, *Inorg. Chem.*, 2013, **52**, 9094–9101.

7 (*a*) E. Deponti, A. Luisa, M. Natali, E. Iengo and F. Scandola, *Dalton Trans.*, 2014, **43**, 16345–16353; (*b*) N. Kaeffer, M. Chavarot-Kerlidou and V. Artero, *Acc. Chem. Res.*, 2015, **48**, 1286–1295; (*c*) R. S. Khnayzer, V. S. Thoi, M. Nippe, A. E. King, J. W. Jurss, K. A. El Roz, J. R. Long, C. J. Chang and F. N. Castellano, *Energy Environ. Sci.*, 2014, **7**, 1477–1488; (*d*) K. J. Lee, B. D. McCarthy, E. S. Rountree and J. L. Dempsey, *Inorg. Chem.*, 2017, **56**, 1988–1998; (*e*) A. Lewandowska-Andralojc, T. Baine, X. Zhao, J. T. Muckerman, E. Fujita and D. E. Polyansky, *Inorg. Chem.*, 2015, **54**, 4310–4321; (*f*) W. K. Lo, C. E. Castillo, R. Gueret, J. Fortage, M. Rebarz, M. Sliwa, F. Thomas, C. J. McAdam, G. B. Jameson, D. A. McMorran, J. D. Crowley, M. N. Collomb and A. G. Blackman, *Inorg. Chem.*, 2016, **55**, 4564–4581; (*g*) D. Moonshiram, C. Gimbert-Surinach, A. Guda, A. Picon, C. S. Lehmann, X. Zhang, G. Doumy, A. M. March, J. Benet-Buchholz, A. Soldatov, A. Llobet and S. H. Southworth, *J. Am. Chem. Soc.*, 2016, **138**, 10586–10596; (*h*) A. Rodenberg, M. Orazietti, B. Probst, C. Bachmann, R. Alberto, K. K. Baldridge and P. Hamm, *Inorg. Chem.*, 2015, **54**, 646–657; (*i*) E. S. Wiedner and R. M. Bullock, *J. Am. Chem. Soc.*, 2016, **138**, 8309–8318; (*j*) D. Z. Zee, T. Chantarojsiri, J. R. Long and C. J. Chang, *Acc. Chem. Res.*, 2015, **48**, 2027–2036.

8 (*a*) F. Gartner, A. Boddien, E. Barsch, K. Fumino, S. Losse, H. Junge, D. Hollmann, A. Bruckner, R. Ludwig and M. Beller, *Chem. – Eur. J.*, 2011, **17**, 6425–6436; (*b*) C. L. Hartley, R. J. DiRisio, M. E. Screen, K. J. Mayer and W. R. McNamara, *Inorg. Chem.*, 2016, **55**, 8865–8870; (*c*) S. P. Luo, E. Mejia, A. Friedrich, A. Pazidis, H. Junge, A. E. Surkus, R. Jackstell, S. Denurra, S. Gladiali, S. Lochbrunner and M. Beller, *Angew. Chem., Int. Ed.*, 2013, **52**, 419–423; (*d*) M. J. Rose, H. B. Gray and J. R. Winkler, *J. Am. Chem. Soc.*, 2012, **134**, 8310–8313; (*e*) Y.-Y. Sun, H. Wang, N.-Y. Chen, A. J. J. Lennox, A. Friedrich, L.-M. Xia, S. Lochbrunner, H. Junge, M. Beller, S. Zhou and S.-P. Luo, *ChemCatChem*, 2016, **8**, 2340–2344; (*f*) P. Zhang, M. Wang, Y. Na, X. Li, Y. Jiang and L. Sun, *Dalton Trans.*, 2010, **39**, 1204–1206.

9 (*a*) H. T. Lei, H. Y. Fang, Y. Z. Han, W. Z. Lai, X. F. Fu and R. Cao, *ACS Catal.*, 2015, **5**, 5145–5153; (*b*) J. Wang, C. Li, Q. Zhou, W. Wang, Y. Hou, B. Zhang and X. Wang, *Dalton Trans.*, 2016, **45**, 5439–5443.

10 (*a*) J. P. Porcher, T. Fogeron, M. Gomez-Mingot, E. Derat, L. M. Chamoreau, Y. Li and M. Fontecave, *Angew. Chem., Int. Ed.*, 2015, **54**, 14090–14093; (*b*) E. J. Sundstrom, X. Yang, V. S. Thoi, H. I. Karunadasa, C. J. Chang, J. R. Long and M. Head-Gordon, *J. Am. Chem. Soc.*, 2012, **134**, 5233–5242.

11 (*a*) G. Li, M. F. Mark, H. Lv, D. W. McCamant and R. Eisenberg, *J. Am. Chem. Soc.*, 2018, **140**, 2575–2586; (*b*) H. Ozawa, M. Haga and K. Sakai, *J. Am. Chem. Soc.*, 2006, **128**, 4926; (*c*) S. Jasimuddin, T. Yamada, K. Fukuju, J. Otsuki and K. Sakai, *Chem. Commun.*, 2010, **46**, 8466–8468; (*d*) H. Ozawa and K. Sakai, *Chem. Lett.*, 2007, **36**, 920–921; (*e*) H. Ozawa and K. Sakai, *Chem. Commun.*, 2011, **47**, 2227–2242; (*f*) C. V. Suneesh, B. Balan, H. Ozawa, Y. Nakamura, T. Katayama, M. Muramatsu, Y. Nagasawa, H. Miyasaka and K. Sakai, *Phys. Chem. Chem. Phys.*, 2014, **16**, 1607–1616; (*g*) K. Yamauchi and K. Sakai, *Dalton Trans.*, 2015, **44**, 8685–8696; (*h*) T. Kowacs, L. O'Reilly, Q. Pan, A. Huijser, P. Lang, S. Rau, W. R. Browne, M. T. Pryce and J. G. Vos, *Inorg. Chem.*, 2016, **55**, 2685–2690; (*i*) M. G. Pfeffer, B. Schafer, G. Smolentsev, J. Uhlig, E. Nazarenko, J. Guthmuller, C. Kuhnt, M. Wachtler, B. Dietzek, V. Sundstrom and S. Rau, *Angew. Chem., Int. Ed.*, 2015, **54**, 5044–5048.

12 (*a*) T. Stoll, C. E. Castillo, M. Kayanuma, M. Sandroni, C. Daniel, F. Odobel, J. Fortage and M. N. Collomb, *Coord. Chem. Rev.*, 2015, **304**, 20–37; (*b*) T. Stoll, M. Gennari, J. Fortage, C. E. Castillo, M. Rebarz, M. Sliwa, O. Poizat, F. Odobel, A. Deronzier and M. N. Collomb, *Angew. Chem., Int. Ed.*, 2014, **53**, 1654–1658; (*c*) H. M. Rogers, S. M. Arachchige and K. J. Brewer, *Chem. – Eur. J.*, 2015, **21**, 16948–16954; (*d*) H. J. Sayre, T. A. White and K. J. Brewer, *Inorg. Chim. Acta*, 2017, **454**, 89–96; (*e*) H. N. Kagalwala, D. N. Chirdon, I. N. Mills, N. Budwal and S. Bernhard, *Inorg. Chem.*, 2017, **56**, 10162–10171.

13 (*a*) S. Tschierlei, M. Presselt, C. Kuhnt, A. Yartsev, T. Pascher, V. Sundstrom, M. Karnahl, M. Schwalbe,

B. Schafer, S. Rau, M. Schmitt, B. Dietzek and J. Popp, *Chem. – Eur. J.*, 2009, **15**, 7678–7688; (*b*) Y. Halpin, M. T. Pryce, S. Rau, D. Dini and J. G. Vos, *Dalton Trans.*, 2013, **42**, 16243–16254; (*c*) J. Prock, C. Strabler, W. Viertl, H. Kopacka, D. Obendorf, T. Muller, E. Tordin, S. Salzl, G. Knor, M. Mauro, L. De Cola and P. Bruggeller, *Dalton Trans.*, 2015, **44**, 20936–20948; (*d*) S. Chen, K. Li, F. Zhao, L. Zhang, M. Pan, Y. Z. Fan, J. Guo, J. Shi and C. Y. Su, *Nat. Commun.*, 2016, **7**, 13169.

14 (*a*) K. L. Mulfort, *C. R. Chim.*, 2017, **20**, 221–229; (*b*) K. L. Mulfort and L. M. Utschig, *Acc. Chem. Res.*, 2016, **49**, 835–843.

15 (*a*) C. V. Krishnan, B. S. Brunschwig, C. Creutz and N. Sutin, *J. Am. Chem. Soc.*, 1985, **107**, 2005–2015; (*b*) M. W. Cooke, D. Chartrand and G. S. Hanan, *Coord. Chem. Rev.*, 2008, **252**, 903–921; (*c*) P. Dongare, B. D. B. Myron, L. Wang, D. W. Thompson and T. J. Meyer, *Coord. Chem. Rev.*, 2017, **345**, 86–107; (*d*) J. Hawecker, J. M. Lehn and R. Ziessel, *Nouv. J. Chim.*, 1983, **7**, 6; (*e*) A. K. Pal and G. S. Hanan, *Chem. Soc. Rev.*, 2014, **43**, 6184–6197; (*f*) L. Petermann, R. Staehle, M. Pfeifer, C. Reichardt, D. Sorsche, M. Wachtler, J. Popp, B. Dietzek and S. Rau, *Chem. – Eur. J.*, 2016, **22**, 8240–8253; (*g*) B. S. O. Rony, S. Khnayzer, K. A. El Roz and F. N. Castellano, *ChemPlusChem*, 2016, **81**, 8; (*h*) E. Rousset, I. Ciofini, V. Marvaud and G. S. Hanan, *Inorg. Chem.*, 2017, **56**, 9515–9524; (*i*) C. V. Krishnan and N. Sutin, *J. Am. Chem. Soc.*, 1981, **103**, 2141–2142; (*j*) A. Zelewsky, A. Juris, V. Balzani, F. Barigelletti, S. Campagna and P. Belser, *Coord. Chem. Rev.*, 1988, **84**, 192; (*k*) M. K. Nazeeruddin, E. Baranoff and M. Gratzel, *Sol. Energy*, 2011, **85**, 1172–1178; (*l*) O. Schott, A. K. Pal, D. Chartrand and G. S. Hanan, *ChemSusChem*, 2017, **10**, 4436–4441; (*m*) M. Rupp, T. Auvray, E. Rousset, G. M. Mercier, V. Marvaud, D. G. Kurth and G. S. Hanan, *Inorg. Chem.*, 2019, **58**, 9127–9134.

16 (*a*) A. Zarkadoulas, E. Koutsouri, C. Kefalidi and C. A. Mitsopoulou, *Coord. Chem. Rev.*, 2015, **304**, 55–72; (*b*) B. Probst, A. Rodenberg, M. Guttentag, P. Hamm and R. Alberto, *Inorg. Chem.*, 2010, **49**, 6453–6460; (*c*) H. Y. Wang, G. Si, W. N. Cao, W. G. Wang, Z. J. Li, F. Wang, C. H. Tung and L. Z. Wu, *Chem. Commun.*, 2011, **47**, 8406–8408.

17 (*a*) P. N. Curtin, L. L. Tinker, C. M. Burgess, E. D. Cline and S. Bernhard, *Inorg. Chem.*, 2009, **48**, 10498–10506; (*b*) B. F. DiSalle and S. Bernhard, *J. Am. Chem. Soc.*, 2011, **133**, 11819–11821; (*c*) A. Jacques, O. Schott, K. Robeyns, G. S. Hanan and B. Elias, *Eur. J. Inorg. Chem.*, 2016, **2016**, 1779–1783; (*d*) C. Lentz, O. Schott, T. Auvray, G. Hanan and B. Elias, *Inorg. Chem.*, 2017, **56**, 10875–10881; (*e*) J. A. Porras, I. N. Mills, W. J. Transue and S. Bernhard, *J. Am. Chem. Soc.*, 2016, **138**, 9460–9472; (*f*) S. Schönweiz, S. A. Rommel, J. Kìbel, M. Micheel, B. Dietzek, S. Rau and C. Streb, *Chem. – Eur. J.*, 2016, **22**, 4.

18 M. S. Lowry, J. I. Goldsmith, J. D. Slinker, R. Rohl, R. A. Pascal, G. G. Malliaras and S. Bernhard, *Chem. Mater.*, 2005, **17**, 5712–5719.

19 (*a*) L. P. Yu, Z. Z. Huang, Y. Liu and M. Zhou, *J. Organomet. Chem.*, 2012, **718**, 14–21; (*b*) Q. Zhao, S. Liu, M. Shi, C. Wang, M. Yu, L. Li, F. Li, T. Yi and C. Huang, *Inorg. Chem.*, 2006, **45**, 6152–6160.

20 (*a*) M. Zalas, B. Gierczyk, M. Klein, K. Siuzdak, T. Pedzinski and T. Luczak, *Polyhedron*, 2014, **67**, 381–387; (*b*) C. Brotschi, G. Mathis and C. J. Leumann, *Chem. – Eur. J.*, 2005, **11**, 1911–1923.

21 R. D. Costa, E. Orti, H. J. Bolink, S. Graber, S. Schaffner, M. Neuburger, C. E. Housecroft and E. C. Constable, *Adv. Funct. Mater.*, 2009, **19**, 3456–3463.

22 S. J. Liu, Q. Zhao, Q. L. Fan and W. Huang, *Eur. J. Inorg. Chem.*, 2008, **2008**, 2177–2185.

23 E. Rousset, D. Chartrand, I. Ciofini, V. Marvaud and G. S. Hanan, *Chem. Commun.*, 2015, **51**, 9261–9264.

24 S. Geremia, R. Dreos, L. Randaccio, L. Antolini and G. Tauzher, *Inorg. Chim. Acta*, 1994, **216**, 4.

25 C. Lopez, S. Alvarez, X. Solans and M. Font-Altaba, *Inorg. Chem.*, 1986, **25**, 2962–2969.

26 S. Soman, G. Singh Bindra, A. Paul, R. Groarke, J. C. Manton, F. M. Connaughton, M. Schulz, D. Dini, C. Long, M. T. Pryce and J. G. Vos, *Dalton Trans.*, 2012, **41**, 12678–12680.

27 M. Polson, M. Ravaglia, S. Fracasso, M. Garavelli and F. Scandola, *Inorg. Chem.*, 2005, **44**, 1282–1289.

28 M. C. DeRosa, D. J. Hodgson, G. D. Enright, B. Dawson, C. E. Evans and R. J. Crutchley, *J. Am. Chem. Soc.*, 2004, **126**, 7619–7626.

29 M. Licini and J. A. G. Williams, *Chem. Commun.*, 1999, 1943–1944.

30 J. L. Dempsey, B. S. Brunschwig, J. R. Winkler and H. B. Gray, *Acc. Chem. Res.*, 2009, **42**, 1995–2004.

31 A. Kutt, I. Leito, I. Kaljurand, L. Soovali, V. M. Vlasov, L. M. Yagupolskii and I. A. Koppel, *J. Org. Chem.*, 2006, **71**, 2829–2838.

32 M. Schulz, M. Karnahl, M. Schwalbe and J. G. Vos, *Coord. Chem. Rev.*, 2012, **256**, 1682–1705.

33 E. Deponti and M. Natali, *Dalton Trans.*, 2016, **45**, 9136–9147.

34 E. D. Cline, S. E. Adamson and S. Bernhard, *Inorg. Chem.*, 2008, **47**, 10.